75th International Astronautical Congress (IAC), Milan, Italy, 14-18 October 2024.
Copyright ©2024 by the International Astronautical Federation (IAF). All rights reserved.

IAC-24,A6,IP,54,x84856

LEVERAGING EVENT-BASED CAMERAS FOR ENHANCED SPACE SITUATIONAL AWARENESS: A NANOSATELLITE MISSION ARCHITECTURE STUDY

Lara Schuberth*, Vincenzo Messina, Ramón María García Alarcia, Jaspar Sindermann, Kian Bostani Nezhad, Roberto Aldea Velayos, Sofia Lennerstrand, Julie Rollet, Federico Sofio, Alessandro Tinucci Monibas, Leonhard Kessler, Alessandro Golkar

Chair of Spacecraft Systems, Department of Aerospace and Geodesy, Technical University of Munich, Lise-Meitner-Strasse 9, Ottobrunn 85521, lara.schuberth@tum.de.
* Corresponding Author

Abstract

Event-based cameras introduce an innovation in the field of imaging by departing from the conventional frame camera paradigm. These bio-inspired sensors capture per-pixel brightness changes asynchronously, generating a continuous stream of events that encode information such as time, pixel location, and polarity alterations. This departure from traditional imaging methods results in distinctive features including high temporal resolution, a high dynamic range, low power consumption, and minimized motion blur. Additionally, event cameras are ideal for motion-oriented applications as they remove superfluous information, optimizing data generation and algorithmic performance. Such characteristics position event-based cameras as useful tools in challenging scenarios as in the realm of object observation in orbit.

This paper presents a comprehensive mission architecture study for our nanosatellite space mission, called EventSat, that focuses on autonomous object detection, classification, and identification in Low Earth Orbit (LEO). The main objective of the mission is to leverage the unique capabilities of event-based sensors for enhancing Space Situational Awareness and autonomous space operations. The nanosatellite mission aims to demonstrate event-based technology to address the growing challenges of monitoring and understanding objects in space, particularly in the densely populated LEO for the sustained, long-term usage of orbital resources through the technological demonstration of event cameras integrated with onboard AI.

The core components of the proposed mission include the integration of event-based cameras with advanced onboard artificial intelligence (AI) systems. This integration holds the promise of significantly advancing autonomous object detection, classification, and identification techniques in space. The ability to exploit the inherent advantages of event-based cameras, such as high temporal resolution and very high dynamic range, can lead to more accurate and timely Space Situational Awareness. The autonomous onboard AI algorithms can empower data sharing between federated spacecraft for automatic maneuvering and collision avoidance, among others.

Furthermore, this paper delves into preliminary payload parameters and demonstrates the viability to use an event camera payload as a proof of concept on a 6U platform, selecting an initial range of focal length for further investigations. The presented analysis shows what payload parameters will maximize the product of pixel count and number of objects, considering looking directly at known objects or looking for chance encounters. We propose how the payload could be used in space in accordance to the selected parameters and point out further work that will allow us to refine and select from the identified possibilities. EventSat aims to bridge the gap between cutting-edge sensor technology and practical space applications, ultimately fostering advancements in space exploration and surveillance capabilities, and empowering space autonomy for safer and more optimal space operations.

Keywords: Event-based cameras, Nanosatellite mission, Object detection, Space Situational Awareness, Artificial intelligence in space

1. Introduction

Event-based cameras represent an innovation in imaging technology diverging from the traditional frame-based approach by mimicking the way biological vision systems operate. Unlike conventional cameras that capture entire frames at regular intervals, event cameras detect changes in pixel brightness asynchronously, providing data with microsecond-level latency, high dynamic range, and minimal motion blur [1]. These attributes make event cameras particularly well-suited for dynamic environments where high-speed object detection and tracking are essential.

This paper explores the potential of event-based cameras in enhancing Space Situational Awareness (SSA) through a nanosatellite mission designed to detect, identify, and classify objects in Low Earth Orbit (LEO). As space becomes increasingly congested, with the number of satellites and space debris expected to rise

Copyright ©2024 by the International Astronautical Federation (IAF). All rights reserved.

exponentially [2], the need for advanced SSA capabilities has never been more critical. Our mission leverages the unique capabilities of event cameras to address these challenges, aiming to contribute to safer and more efficient space operations.

SSA involves the comprehensive monitoring and understanding of the space environment to ensure the safe and sustainable use of space. In this context, we aim to offer a proof of concept for the use of event cameras for the autonomous detection and classification of space objects. The integration of Artificial Intelligence (AI) onboard the nanosatellite is a key innovation of this mission. AI algorithms will process the event-based data in real-time, enabling rapid identification and tracking of objects, thereby enhancing the satellite's capability to autonomously collect and interpret data of space traffic, potentially avoiding collisions.

To provide a comprehensive understanding of our mission and its underlying technologies, this paper is organized as follows. In Section 2 we begin with an overview of event-based cameras, emphasizing their operational principles, unique advantages, and potential limitations within space applications. This sets the foundation for our subsequent exploration of artificial intelligence integration, where we overview how onboard AI systems process event-based data to enable autonomous object detection, classification, and identification in space. We then present, in Section 3, the mission architecture of EventSat, outlining its objectives, payload and subsystem overview, Concept of Operations, and a comparison with current and planned Space Situational Awareness initiatives. Following this, in Section 4, the payload configuration and preliminary results from our performance analyses on space object detection are detailed. Finally, in Section 5, we delve into the future work necessary to advance this technology, including planned testing and refinement of both the event camera and the onboard AI systems, to ensure our mission effectively enhances Space Situational Awareness.

Through the development and deployment of this mission, we seek to bridge the gap between cutting-edge sensor technology and practical space applications, ultimately fostering advancements in SSA and promoting safer, more autonomous space operations.

2. Background

The operational principle of event cameras differs fundamentally from standard frame cameras. In contrast to standard cameras, event cameras measure logarithmic intensity changes $L \doteq \log(I)$, also called brightness changes for every pixel asynchronously and independently. By exceeding a threshold $\pm C$ each pixel $\boldsymbol{x_k} \doteq (x_k, y_k)$ sends an event $e_k \doteq (\boldsymbol{x_k}, t_k, p_k)$, resulting in a stream of events that logs the location, time, and the polarity $p_k \epsilon \{+1, -1\}$, which indicates the alteration of sign of the brightness [1].
Hence, compared to frame cameras, which contain data from every pixel in the frame and therefore carry redundant information, event cameras do not and instead result in a frame-free output with a high temporal resolution and dynamic range, 120-130 dB for typical neuromorphic sensors [3].

The advantages of event cameras are evident in the high temporal resolution, facilitating the tracking of high-speed motions without encountering motion blur, the latency, the low power consumption, and the high dynamic range [1]. These advantages not only render event cameras particularly interesting for applications in robotics and computer vision, where conventional cameras encounter limitations [1], but also for applications of Space Situation Awareness [4]. The high temporal resolution and low latency allow a rapid observation of targets and a rapid response to other newly appearing Resident Space Objects (RSO's) [4]. The camera is able to detect small differences in luminance with respect to objects varying in speed, making the sensor particularly suitable for space-based imaging [5].

However, as the generation of events results from moving edges of an object, event cameras only picture object edges, leaving much of the scene's information uncaptured [6], which makes the classification and identification of space object more challenging. In addition, event cameras are prone to background noise caused by transient disturbances and leakage currents in semiconductor PN junctions due to the sensor's design. The noise level increases in low-light conditions or when the camera's sensitivity is set higher. A limitation can be also seen in the pixel size of event cameras. The pixel size is often bigger in comparison to available industrial frame cameras, which are ranging of 2~4 µm of pixel size, resulting in a smaller resolution of event cameras. Additionally, the fill factor, which represents the ratio of the light sensitive area of a pixel to the total area, is small [6].

There have already been studies on event cameras for space applications. Existing work looks at star tracking to overcome star tracker limitations of slow rotational speeds and large power consumption [3] [7] [8] [9], satellite pose estimation based on event data [10], and satellite material characterization [11]. In addition, previous work considered vision-based exploration on Mars helicopter missions [12] and event-based spacecraft landing on the Moon [13]. On the "M2" CubeSat mission of the Western Sydney University, UNSW Canberra Space and the Royal Australian Air Force, the DAVIS240C event camera, supplied by iniVation,

Copyright ©2024 by the International Astronautical Federation (IAF). All rights reserved.

became in 2021 the first event camera launched into space [14]. In a cooperation of the Western Sydney University's International Center for Neuromorphic Systems and the United States Air Force's Academy Space Atmospheric Research Center, two iniVation DAVIS240C event cameras were launched to the International Space Station (ISS) in December 2021 [15]. For ground-based object detection and tracking, the Western Sydney University's International Centre for Neuromorphic Systems (ICNS) equipped telescopes with iniVation's DVS346 event camera and Prophesee's Gen 4 HD within the project AstroSite-1 and AstroSite-2 [4].

The need for enhanced Space Situational Awareness systems and autonomous satellite operation rises from the growing number of objects in space. As stated in a review article from 2020 by Abid Murtaza et al. [2], most objects found in Low Earth Orbit are orbiting in the 800-1,000 km range. Next to active satellites, several types of objects are found in Low Earth Orbit. As of June 2024, the Space Debris Statistics released by ESA has found it to currently be 22,019 cataloged manmade objects orbiting in LEO which can be traced back to a launch event, counting the non-traceable non-cataloged objects this number is expected to be significantly higher [16]. These objects can all be tracked back to a launch event and include space objects designed to perform a specific function excluding a launching function (denoted as Payloads), objects released as space debris after serving a mission function (Payload mission related objects), unintentionally released objects which can be traced back to the release event/belonging of which spacecraft (Payload fragmentation debris), unintentionally released objects which cannot be traced (Payload debris), objects designed for launch related performances (Rocket body), intentionally released objects which served purposes for a rocket body (Rocket mission related objects), unintentionally released objects from a rocket body which can be traced (Rocket fragmentation debris) and lastly unintentionally released untraceable objects from a rocket body (Rocket debris) [16]. Other non-manmade objects to be potentially (rarely) found in LEO are Near Earth Objects (NEOs), which are essential to detect since they pose a threat to life on Earth. Most NEOs are asteroids according to the statistics released by NASA's Center for Near Earth Object Studies [17].

The usage of onboard AI can be seen as one of the enablers for enhanced Space Situational Awareness systems and autonomous satellite operation. As of now, the use of artificial intelligence onboard satellites has become a rampant trend. Although there are limitations, such as limited processing capabilities due to radiation-hardened hardware. Other limitations include difficulties training an AI algorithm with a simulation of real-time data, the demand of a GPU creates excess heat due to high power consumption and is usually not radiation hardened [18]. By using an onboard AI, the downlink data could be reduced significantly, as an example the CubeSat PhiSat-1 managed to reduce its downlink data 90% in 2020 [19].

Waseem Shariff et al. demonstrated object detection on event-based vision data in the automotive field [20]. N. Salvatore and J. Fletcher [5] adapted this algorithm to object detection in LEO via telescope observations utilizing an event camera. Furthermore, N. Salvatore and J. Fletcher simulated their own event-based training dataset with satellites in LEO as motives, in this way they trained a YOLO-based object detection model to detect objects in space specifically. The YOLO model was first proposed by Redmon et al. [21] in 2016 and has 24 convolutional layers and 2 fully connected layers and into a single volume it combines feature extraction, regression and classification. The YOLO model has achieved state-of-the-art performance in real-time object detection, on the other hand it does not perform as well on detecting small objects [22].

3. Description of the mission

The nanosatellite mission EventSat, consisting of a 6U CubeSat operating in Low Earth Orbit with an event camera payload, aims for demonstrating event vision for space-to-space object observation.

In this section, we present a description of the EventSat mission. We cover its objectives and main high-level requirements, a block diagram depicting the mission architecture, a Concept of Operations (ConOps), with a focus on the usage of Artificial Intelligence, and finally a comparison with current and planned Space Situational Awareness missions for object detection, identification and classification.

3.1 Mission statement, mission objectives and mission requirements

The mission of EventSat is to advance autonomous object detection, classification, and identification techniques in space for enhanced Space Situational Awareness and autonomous space operations, through the technological demonstration of event cameras integrated with onboard AI.

In particular, the mission statement breaks down into the following mission objectives:

1. To study and develop AI-based autonomous object detection, classification, and identification algorithms suited to event cameras' output.

2. To design, build, and test a 6U CubeSat (EventSat) with an event camera and an onboard AI PC payload.

Copyright ©2024 by the International Astronautical Federation (IAF). All rights reserved.

3. To procure the launch to orbit (LEO or SSO, 400 to 600 km) and operate the CubeSat in orbit to technically demonstrate the developed hardware and software.

4. To prove the techniques in orbit for nearby (<500 km) satellites and bigger objects (asteroids, comets).

5. To analyze the results for future improvement and for scientific publication and dissemination.

6. To decommission the satellite safely with end-of-life.

The mission objectives synthesize into a series of high-level mission requirements that inspire the design decisions taken. In particular, the mission shall detect objects in space autonomously, shall classify them, and shall identify them. Thereby, the mission shall demonstrate the use of event cameras in space and shall demonstrate the use of onboard AI as well for object detection, classification, and identification in space. Additionally, the mission shall downlink detection, classification, and identification reports in regular ground station passes, and shall be able to be reconfigured by AI model update through telecommand. Regarding the satellite, the mission's satellite shall be in the form of a 6U CubeSat, shall operate in a LEO or SSO between 400 km and 600 km, shall not consume more than 50 W and shall not weigh more than 12 kg. Finally, the mission shall comply with applicable end-of-life disposal regulations.

3.2 Mission architecture

The mission architecture outlines the design, structure, and functionalities for satisfying the requirements and achieving the mission objectives. This is essential to make sure that the satellite operates as desired and can contribute to improving the state of the art of autonomous object detection using nanosatellites with event-based camera technology.
Figure 1 illustrates a block diagram of the satellite system architecture.

The CubeSat is housed within a 6U structure, which refers to a standardized unit used for CubeSats. The 6U structure measures around 10x20x30 cm and provides space for the satellite's components. The power subsystem powers all the other subsystems, with power connections represented by the red arrows. Then the Computer and Data Handling acts as the central processing unit, managing data from, and to, various subsystems and controlling the satellite's operations; with blue arrows showing the data interfaces. Additionally, the Attitude Determination and Control Systems (ADCS) is responsible for determining and controlling the satellite orientation in space. It receives power and data from the power subsystem and computer subsystem. The communication subsystem handles all communications between the CubeSat and the Ground Station, and is also connected to both the power and computer subsystems to ensure smooth data transmission and reception. It is important to underline that the Ground Station and Mission Control Center are located in the facilities of the Technical University of Munich, and they are managed by the Chair of Spacecraft Systems.

Lastly, the payload components are represented with green boxes, and they relate to power and data interfaces to the rest of the spacecraft, to guarantee the correct operation of the payload. Section 3.2.1 presents more details on the payload.

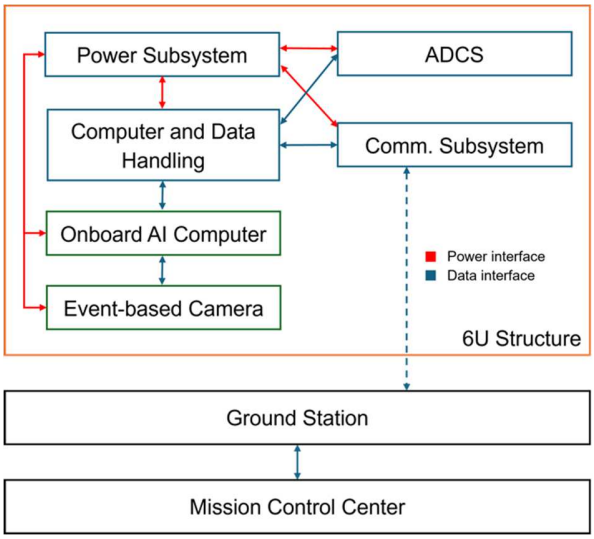


Figure 1: Block diagram showing EventSat system architecture

3.2.1 Payload

The main driver of the mission is the payload, including the imaging payload, with the event-based camera and optic, and onboard AI computer. The event camera specializes in the detection of fast-moving objects. The design of the imaging payload considers the types of objects detected in space, such as active satellites, debris, and meteoroids. The team designs the optics and integrates the event-based sensor to enhance the mission's observation capabilities. The aperture diameter is set at 90 mm due to the size constraints of the CubeSat structure and its mechanical supports. This setting affects the diffraction limit and, consequently, the minimum target size the camera can detect. The CubeSat dimensions and the 2U space allocated for the payload determine the maximum focal length. This limits the physical size of the payload; hence we selected a Cassegrain configuration to obtain a larger focal length with a smaller size. Below this hard limit, we study the

Copyright ©2024 by the International Astronautical Federation (IAF). All rights reserved.

effects of the dimension of the focal length on the detectable objects and Section 4 presents its results.

We chose the NVIDIA Jetson Orin Nano [23] as AI onboard computer (AI-OBC) because of its wide availability, community and support. The structure also encloses the AI-OBC to interface the imaging payload with the rest of the satellite and operate the algorithms of detection, classification, and identification of the objects.

3.2.2 Subsystems Overview

This overview highlights the different subsystems of EventSat. The power subsystem utilizes body-mounted solar panels across the entire surface of the CubeSat. It also includes a power management unit with two battery packs, providing a total capacity of 168 Wh.

The communication subsystem consists of a UHF antenna and transceiver for telemetry and command operations. It is also responsible for transmitting science and payload data. Due to the volume of data, a higher data rate is required, so an additional X-band antenna and transceiver are included.

The attitude determination and control subsystem integrates an ADCS with one star tracker aligned with the payload, two sun sensors, and a 3-axis magnetometer for determining attitude. It also employs four reaction wheels, one of which is redundant, along with magnetorquers to control attitude. This setup ensures precise pointing of the event camera to help determine the position of detected objects, while the actuators facilitate pointing and tracking maneuvers as needed.
The satellite is planned to operate without a propulsion subsystem. Further analysis is required to determine if any passive thermal control elements are necessary.

3.3 Concept of Operations (ConOps)

The Concept of Operations (ConOps) for EventSat defines the activities and operations from launch to the satellite's decommissioning. After deploying the CubeSat in Low Earth Orbit at an altitude of around 550 km, chosen for the ease of finding launch opportunities and the higher satellite density, the mission will enter the initial commissioning phase. During this phase, the team will activate and, if necessary, calibrate and test all subsystems and payloads, including the event camera and onboard AI computer.

Once the commissioning phase ends, the operational phase will begin. During this phase, the camera will capture images of deep space when the available onboard power exceeds a specific threshold. This step will help create a database of stars observed by the event camera in space, and it will detect satellites, debris, or natural objects. The onboard AI computer will process this data in real-time to detect, classify, and identify objects in space. The team will then transmit the processed data to ground stations for further analysis.

Throughout the mission, the team will adjust the camera's sensitivity and software biases based on the camera's behavior in space and detection capabilities. Constant communication to send telemetry will be crucial for ensuring mission integrity and achieving objectives.

At the end of the mission, EventSat will undergo decommissioning operations to ensure an uncontrolled re-entry in line with space debris mitigation regulations.

3.4 Usage of Artificial Intelligence

The usage of Artificial Intelligence to process the data gathered by the event camera payload and detect, classify, and identify objects, is one of the innovations of the EventSat mission.

We plan on using Convolutional Neural Networks (CNN), a type of Deep Learning (DL) architecture particularly used for object classification in terrestrial applications. The models will be trained on the ground using real data from space catalogs and synthetically generated data, then uploaded to the NVIDIA Jetson Orin Nano computing payload. The models will run using the Pytorch package within the Python programming language, leveraging the CUDA library for GPU acceleration provided by NVIDIA, all while maintaining a relatively low power consumption of around 10 W.

Due to the capability to upload and run new code enabled by the Jetson's Operating System and software architecture, the CNN models might be further trained on the ground, upgraded and uploaded whenever new quality data becomes available. We will explore the vision transformer architecture for potential use, following emerging trends in AI. Although training will primarily take place on the ground, due to the higher computational power and reduced training time available there, EventSat will also demonstrate onboard model training or refinement. This capability will allow for even greater autonomy in space as new data is produced during the mission.

3.5 Comparison to other current and planned missions

This subsection locates the EventSat mission within a broader context by delving into the current and future space-to-space object detection missions and outlining the similarities and differences with our proposal.

Earth's orbit, and very particularly Low Earth Orbit, is getting increasingly populated in the recent years, due to the progressive deployment of mega constellations, the most prominent being Starlink [24] by SpaceX, with other examples found in OneWeb [25] or Project Kuiper [26].

Copyright ©2024 by the International Astronautical Federation (IAF). All rights reserved.

The trend towards more crowded orbits comes with an increase of the collision probabilities and an awareness of the need of establishing proper Space Situational Awareness and Space Traffic Management (STM) systems. While these systems primarily operate from the ground through telescopic sky monitoring [27], there is growing consideration for an orbital component. On the commercial side, several proposals are gaining traction and receiving both private and institutional funding.

Table 1: Comparison between EventSat and other in-space SSA missions

Mission	Satellites	Resolution	Technology
EventSat	1	15 cm at 500 km	Event-based
Skylark (NorthStar)	12 (option for 18 more)	> 5 cm in LEO > 40 cm in GEO	Classical, frame-based
Flamingo (Vyoma)	12	> 10 cm in LEO	Classical, frame-based
SBSS (ESA/GMV)	4	> 70 cm in GEO	Classical, frame-based

The most prominent example is the Skylark constellation of the Canadian company NorthStar, which has started putting in place the first SSA constellation. Placed in LEO, it currently has four satellites in orbit out of the twelve planned (expandable to thirty). These satellites orbit at 520 km altitude with a 97.48-degree inclination, using traditional frame-based optical telescopes to detect objects larger than 5 cm in LEO [28].

Another example is the German firm Vyoma, that has recently commissioned the construction of two small satellites for a constellation called Flamingo, composed of up to twelve satellites in LEO to observe objects in space. The initial two satellites will detect and catalog objects larger than 10 cm in LEO, while subsequent satellites will detect objects down to a few centimeters, also using traditional frame-based optical telescopes [29] [30].

Interest also exists on the institutional side. In 2017, as part of an assessment study financed by ESA, GMV presented an initial study for the so-called Space Based Space Surveillance (SBSS), for the observation of objects larger than 70 cm in the GEO region. An initial demonstration mission with the SBSS-DM satellite would be completed by a final constellation of 4 SBSS satellites. While compared to the previous commercial missions the focus is more on the GEO region, the proposal still boasts classical, frame-based optical telescope, in this case a Ritchy-Chrétien one with a CMOS sensor [31].

Spire Global produces the satellites of Skylark and they are 16U CubeSats of the Lemur-2 series [32]. Endurosat built Flamingo 1 based on its ESPA platform [29] [33]. The satellite has a mass between 70 and 150 kg, volume of about 50 x 50 x 65 cm, and power consumption between 60 and 200 W. Aerospacelab built Flamingo 2 based on the VSP-150 platform, with a mass between 150 and 250 kg, volume of 50 x 50 x 50 cm, and power consumption between 50 and 300 W [30] [34]. QinetiQ Space built the SBSS satellites, with a mass around 170 kg, volume around 140 x 90 x 90 cm, and power consumption between 160 and 200 W [31].

Table 2: Comparison between EventSat and other SSA satellites

Satellite	Mass [kg]	Volume [cm]	Power [W]
EventSat	9	6U	19
Skylark 1-4	n.a.	16U	n.a.
Flamingo 1	70 – 150	50 x 50 x 65	60 – 200
Flamingo 2	150 – 250	50 x 50 x 50	50 – 300
SBSS	170	140 x 90 x 90	160 - 200

In comparison, EventSat is a smaller satellite, a 6U CubeSat of mass 9 kg, volume of 6U, and power consumption between 7 and 19 W, achieving similar resolutions to the compared missions. This is possible due a compromise on the object resolution, and particularly by the usage of the event-based vision, which greatly reduces the power consumption and allows the payload to fly on smaller platforms. By demonstrating the feasibility of a smaller platform, EventSat will eventually contribute to a quicker, more cost-effective deployment of in-orbit SSA systems.

4. Payload configuration and performance analysis

This analysis serves to assess the viability and performance of a CubeSat sized event camera payload for Space Situational Awareness within the restriction of the EventSat mission. The goal of this analysis is thus:

1. To justify that a CubeSat event payload would be able to see and detect RSO's.
2. Achieving a payload configuration which will best identify and classify RSO's.
3. Identifying payload aspects needing further development.

The payload performance will be evaluated for focal lengths ranging from 100 mm to 1,000 mm, as this focal length range is considered achievable for a 2U payload.

The spacecraft's form factor predetermines the payload parameters such as aperture size of the optics, however, arriving at usable focal lengths for the payload optics is perhaps the most important undecided parameter

Copyright ©2024 by the International Astronautical Federation (IAF). All rights reserved.

which this analysis intends to determine. The distances between the observing payload and the space objects of interest are difficult to model and depend on the orbits of EventSat and every other object in LEO. This analysis thus evaluates the payload performance for different distance ranges.

The analysis consists of two parts. We first compare expected payload performance against known artificial space objects in LEO. Known artificial space objects are objects which are tracked and available in public catalogues. An object being tracked implies a satellite and the payload can be purposefully pointed at it. The second part is on the expected detection rate of so-called chance encounters. Chance encounters happen when the payload is pointed in an arbitrary direction with the hopes of observing passing objects.

Both parts of the analysis require knowledge about two main properties of RSO's that decide their observability. The two relevant properties are their sizes and their reflectivity. For the study, we determine the expected sizes of the objects with existing catalogues. The reflectivity of an object, which is a surface material property, is harder to find and often not shared. This ambiguity on the surface materials of RSO's is especially relevant for space debris with uncertain origins. Thus, we assume a reflectivity of $\Gamma = 0.15$, equivalent to the reflectivity of solar panels [35] for the observed objects in the analysis. This assumption is made since solar panels usually make up the largest surface area of any artificial satellite.

The main assumption of this analysis is on the sensitivity of the event sensor to low light events. At some point, objects will be so faint that they present no detectable contrast to either the observed background or the noise floor of the event sensor. The assumption states that the camera can detect objects with a brightness of no less than 10 visual magnitudes ($m_{obj} > 10$). This is based on telescopic observations performed with a DAVIS event camera using a 90 mm aperture telescope [36].

In addition, the analysis is limited to objects in LEO with orbits below 1,000 km perigee.

4.1 Performance with known artificial space objects

This first part of the analysis is on comparing payload performance against known artificial space objects. More specifically, determining if detections are feasible and which focal length configurations will aid in detection, classification, and identification.

Known artificial space objects are human-made objects which are tracked, for example, by the US Space Force. In this analysis, we derive the sizes of known objects from the General Catalogue of Artificial Space Objects (GCAT) [37]. This catalogue contains a comprehensive record of objects in LEO, together with their known or estimated sizes. However, the catalogue does not indicate sizes of objects smaller than 10 cm, which thus the analysis does not consider.

The payload performance against known artificial space objects is evaluated by finding the distance at which objects are observable whilst taking the positional errors of the objects into account. The positional errors of the objects and their maximum observable distance affect the choice of focal length for the payload. The performance is evaluated for a range of distances, where the visibility of each catalogued object is determined for every considered distance.

The brightness in units of visible magnitudes of a space object in LEO m_{obj}, illuminated by the sun, is given the following equation [35]:

$$m_{obj} = -26.78 - 2.5 \cdot log_{10}\left(\frac{\Gamma \cdot A \cdot p_{\phi}}{d^2}\right) \quad (1)$$

The first term of the formula is a constant related to the visible magnitude of the Sun at Low Earth Orbit. Γ, in the second term, is the reflectivity of the object, A is the surface area of the object, p_{ϕ} is the phase function of the object, and d is the distance between the observing payload and the observed space object. The phase function describes the amount of light reflected from an object, depending on the object's shape, and the angle ϕ between the object and the observer as seen from the object. The phase angle ϕ is important determining the observability of an object. The observed object is the brightest at complete opposition, i.e. when the observer is directly between the object and the sun. The brightness decreases as the phase angle grows, until the object is between the sun and the observer, at which point it is impossible to see it. This analysis applies a simplification and assumes all objects to be spheres which are observed at complete opposition. This gives a constant phase function of: $p_{\phi} = 0.21$.

.

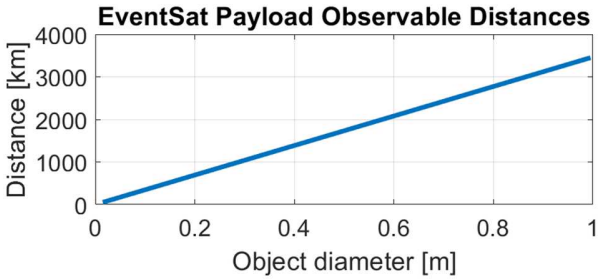


Figure 2: Observable distances for object sizes up to 1 m in diameter.

Equation 1 can be used to determine observable distance for different object sizes. Figure 2 shows e.g. the observable distances of objects up to 1 m in diameter, assuming a 10 visible magnitude payload sensitivity limit.

Copyright ©2024 by the International Astronautical Federation (IAF). All rights reserved.

Known objects usually have their orbital parameters published as Two-Line-Elements (TLEs) which can be used to determine where to point the observing payload. These TLEs are subject to inaccuracies in the order of several kilometers. Furthermore, TLEs are merely a snapshot in time, and orbital perturbations will amplify the error with time. The errors of the objects of interest are there for important to estimate.

We use the results of R. Wang et al. [38], which provide the expected one-day TLE errors for different orbits, to estimate positional errors. We linearly extrapolate their results to find the one-day error for every catalogued object of interest, as shown in Figure 3. The positional error increases for lower orbits, which is due to the increased atmospheric drag.

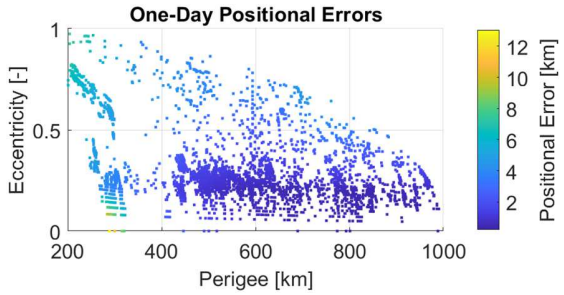


Figure 3: One-day positional errors of known artificial space objects.

As shown in Figure 4, we assume the positional error of each object ϵ_{obj} to be the radius of a sphere. The sphere contains all the possible positions of the object. The origin of the sphere is the object's expected position. The probability of detection is given by how much of the potential object positions are covered by the field of view of the observing payload. Additionally, the positional error of the observing payload ϵ_{obs} could be considered, should it be non-negligible. This consideration could be relevant if the observing satellite does not carry a GNSS receiver or other positioning systems, since then it would be tracked using TLE's as well with the accompanying errors. For the purposes of this analysis, we assume the position of the observing payload to be accurately known. The potential object positions span a volume, and thus the probability is largest, when more of that volume is covered by the observing payload field of view. The largest volumes are in the center of the sphere as seen from the observing payload. As the field of view expands, the additional gain in volume diminishes until the whole sphere is covered by the payload field of view. The detectability of objects is thus dependent on the field of view of the observing payload. The field of view is in turn dependent on the focal length of the payload optics. A longer focal length results in a smaller field of view. However, a longer focal length also offers better magnification. This presents a trade-off, where the number of possible observations must be balanced with the quality of observations. More objects can be reliably seen despite large positional errors, if the field of view is large. Higer quality observations can be made if the magnification is larger.

In addition, the pointing errors of the observing satellite could be considered. The pointing deficiencies of the ADCS subsystem need to be considered in any in-depth analysis of the payload. For the sake of simplicity, this is excluded from this analysis.

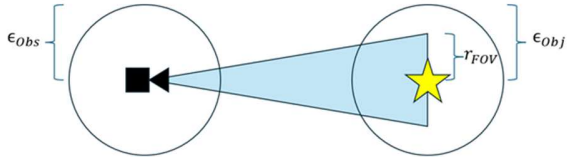


Figure 4: Errors around observer and objects.

Building on these findings, it is possible to determine how distances and focal lengths affect the observability of RSO's. The probability of detection for each object is found for every focal length and distance based on the positional errors. The analysis determines the sum of objects with a probability higher than the threshold. As a starting point, we selected a high probability of detection of 80%. All catalogued objects larger than 10 cm are considered for distances up to 3,000 km. The results are shown in Figure 5.

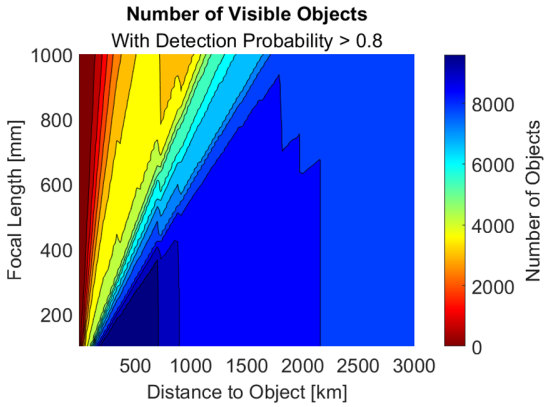


Figure 5: Number of visible known artificial objects as a function of distance to observer and focal length.

The figure also takes the observable distance of every object regarding brightness into account. The visible jumps in the contours result from groups of objects that become too faint to see. Closer study of the catalogue shows that the jumps are often constellations of the same satellite type with similar sizes which disappear. It can also be seen that the long focal lengths are detrimental at close range due to the positional errors. It is therefore beneficial to have a short focal length, if more objects are to be seen.

Copyright ©2024 by the International Astronautical Federation (IAF). All rights reserved.

Based on the magnification of the payload optics, we calculate the number of pixels that each space object has on the sensor. The magnification is in turn calculated from the focal length. Assuming the camera sensor is in the focal plane, the transversal magnification M_T is given by the distance to the object d_{obj} and the focal length f [36]:

$$M_T = -\frac{f}{d_{obj}} \qquad (2)$$

The size of the object image on the focal plane h_{img} can be found using the actual size of the object h_{obj}:

$$h_{img} = M_T \cdot h_{obj} \qquad (3)$$

To determine the pixel size of each object, the size of the object image is divided by a pixel size of the sensor. For the study, we assume a pixel size of 4.86 µm, corresponding to the pixel size of the Sony IMX636 event sensor [39]. Applying these calculations, we determine the average pixel count of all catalogued objects for every combination of focal length and distance, as shown in Figure 6.

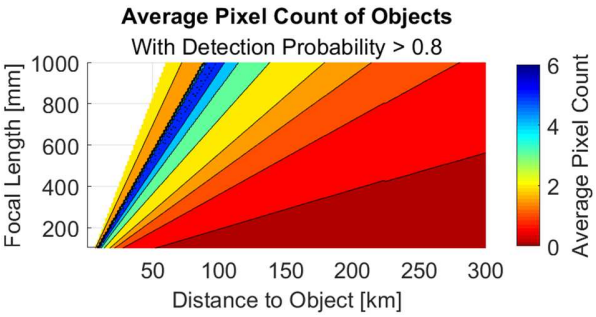


Figure 6: The average pixel count of all catalogued objects as a function of distance and focal length.

Figure 6 shows that anything larger than a single pixel is only achievable with long focal lengths and short distances below 100-150 km. The average pixel count is the quality of the detection. Detections may be missed as single pixels could be mistaken for noise. Reliable detections are necessary for identifying and classifying objects.

In conclusion, for the detection of known objects, the mission would benefit from a wide-angle optics, with a low focal length. This would ensure that more objects can be seen, despite their positional errors, especially when the errors have propagated. This would however reduce the quality of those detections, since the pixel count would be smaller. An important note on this part is that the number of visible objects falls drastically when the distance becomes shorter, due to positional errors, as shown in Figure 5. This exaggerates the average number of pixels per object for short distances. This can be seen in Figure 7 which shows the product of the average pixel count and number of objects. This product is a combination of the two metrics used to find optimal distances and focal lengths. The product shows two areas of interest. The first is the red area for short distances where the product is very small, since few objects are visible despite their high pixel counts. The second area is the dark blue line correlating certain distances with certain focal lengths. This dark blue area is where the highest combination of pixel and object count is achieved and can thus be considered an optimum.

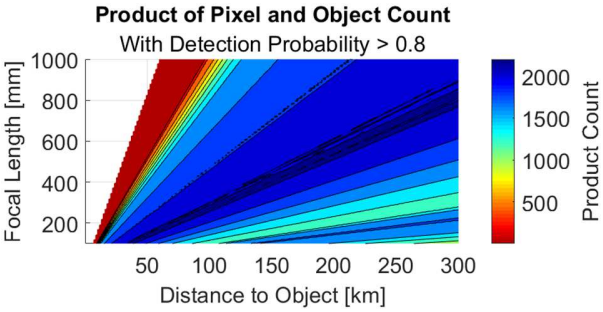


Figure 7: The pixel and object count products as a function of distance and focal length.

Figure 8 shows that accepting a lower probability of detection results in higher pixel and object count products. This means that higher quality observations can in be made on more available RSO's. This indicates a trade-off between certainty of observations and quality and abundance of observations.

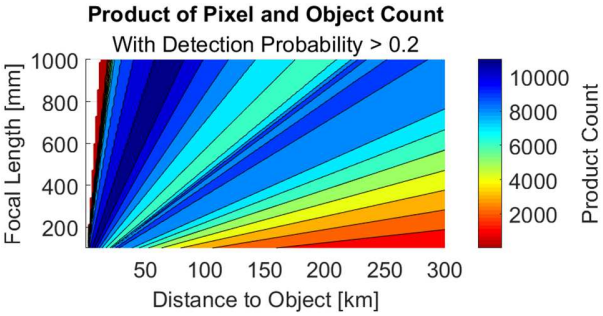


Figure 8: Pixel and object count product with reduced detection probability.

4.2 Chance encounters

In comparison to the previous section, which examined the payloads performance in detecting known objects to which the payload is purposefully pointed at, this section focuses on the payload's ability to record chance encounters of space objects and debris. In a first step, we identify the density of RSO's in LEO. We then account the expected brightness of these objects with Equation 1, to determine the distance limits. Lastly, we derive the number of chance encounters.

Copyright ©2024 by the International Astronautical Federation (IAF). All rights reserved.

We determine the density of space objects in LEO using the ESA Master software [40]. The spatial density is found for object sizes 0.01 m to 1.0 m at an altitude up to 1,000 km. The spatial densities are shown in Figure 9. It is clearly visible that the density falls sharply with size.

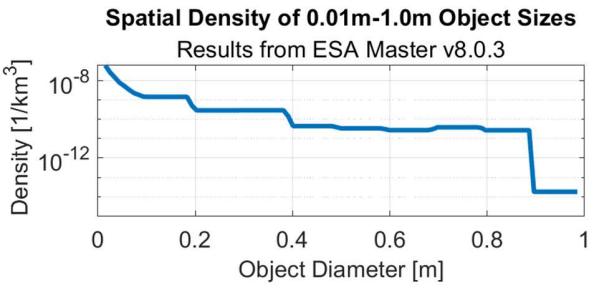


Figure 9: Spatial density of objects with sizes from 0.01m to 1.0m. Figure derived from ESA Master.

We evaluate the visibility of chance encounters with Equation 1 by assuming again full opposition and a reflectivity of $\Gamma = 0.15$. This time however, we reverse Equation 1, such that the maximum visible distances are determined from the payload magnitude limits and object sizes.

For this part, the analysis considers the volume of the field of view of a camera as a pyramid with a rectangular base, as shown in Figure 10. The maximum observable distance of objects is the height of the pyramid. The payload is at the apex of the pyramid. The pyramid volume increases when the field of view and observable distances increases.

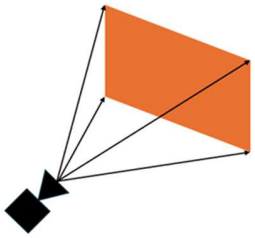


Figure 10: The volume covered by a camera's field of view is a pyramid, with the camera at the apex.

An expression for the pyramid volume based on distances to objects and the focal length can be derived by including an expression for the pyramid base area using the angle of view:

$$V = \frac{4}{3} \cdot tan^2(\varphi) \cdot d^3 \quad (4)$$

where φ denotes the angle of view of the camera derived from the focal length. The distance d is the distance where objects become too faint to see. The volume of the pyramid at a given focal length can be used, together with the spatial density estimated using ESA Master, to find the instantaneous number of encounters in view for objects of different sizes. Considering the spacecraft velocity in a 550 km LEO orbit allows to find the hourly encounters as shown in Figure 11.

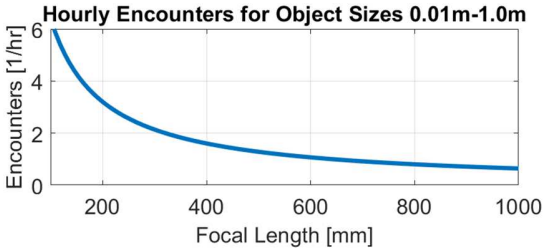


Figure 11: Hourly encounters for all object sizes.

Figure 11 shows multiple hourly encounters, especially for short focal lengths. Consequently, it is likely that the payload will have chance encounters, especially over time. However, the encounters are calculated assuming favorable conditions. Lighting conditions and incidence angles would in reality make the observing of objects more difficult. In conclusion, a short focal length aids detecting chance encounters. The quality of the encounters is, however, uncertain.

4.3 Payload performance summary and discussion

In the following section, we summarize the conclusions on the payload performance and focal length of the EventSat mission.

The first and main conclusion is that EventSat will be able to see thousands of objects at several thousands of kilometers. More objects will be visible with a short focal length. Concretely, as shown in Figure 2, 15 cm diameter LEO objects are visible until 500 km. It must be added that object visibility depends on lighting conditions and phase angle. The analysis assumes ideal conditions so far. Fewer objects would be visible. Furthermore, only short distance observations of 100-150 km with a long focal length (>500 mm) would yield observations larger than a single pixel. This can be mitigated by accepting a lower detection probability to achieve higher quality detections and more visible objects. The final conclusion is, that EventSat would, with a short focal length below 200 mm, experience a rapid increase in chance encounters every hour.

These results are encouraging and show that EventSat would be able to perform SSA observations despite its limiting CubeSat formfactor. The extent and quality of the observations would be subject to further work. We can derive three payload strategies for further development and use of the payload from the current results. A final strategy can be developed once further development has been completed.

The first strategy is named *Search Maneuvers*. This strategy requires a high-precision ADCS subsystem and

Copyright ©2024 by the International Astronautical Federation (IAF). All rights reserved.

an equally capable power subsystem. With a capable ADCS system, the spacecraft could perform slew maneuvers to search a potential target area. This allows for a long focal length at the cost of added mission complexity. The necessary observation time may also be longer due to the search, adding additional power consumption. The analysis shows that objects can be seen with a higher pixel count, if a lower detection probability is acceptable. The lower probability would be offset by a search. The probability of detection is dependent on the field of view. Moving the spacecraft to cover a larger area, compensates for a small field of view which is necessary for larger magnification and thus increases the probability of detection. Here the longest focal length supported by the pointing accuracy of the ADCS subsystem is chosen.

The second strategy is called *Proof of Concept*. This strategy applies a long focal length, same as the previous strategy. Instead of performing search maneuvers this strategy aims to target objects whose positions are well understood and tracked. This requires tracking data from external sources or agencies, which are better than generally available TLE's. The strategy is called "*Proof of Concept*" as it aims to be just that. Potential resource and development limitations may not allow for the needed ADCS and power storage capabilities to perform searches. Instead, by targeting well tracked objects, the merits of event cameras for Space Situational Awareness could be proven and knowledge gathered for future missions with more capabilities.

The last strategy is called *Large Field of View (FOV)*. This strategy is the least complicated of the three. A short focal length is chosen, which allows for a large field of view. It would ensure objects can be seen despite their positional errors, however with a lower pixel count. In this strategy, the smallest practically feasible focal length would be chosen. The ratio of focal length to aperture diameter would need to be large enough to avoid distortions and aberrations. This strategy has the added benefit of being less sensitive to pointing errors of the ADCS subsystem. It would also be less sensitive if correct positioning of the observing satellite isn't possible, for example if it does not have a GNSS receiver onboard.

5. Limitations and Future work

In this section, we cover the limitations and the future planned work. The future work includes tests to enhance our assumptions on the event camera to refine the mission and payload architectures and designs.

Besides the presented advantages of event cameras, we identify the increase of the noise level in low light-lighting conditions as a possible limitation for the EventSat mission. This limitation becomes especially relevant when objects are so distant or small that they only generate events of a single pixel or a few pixels on the sensor. One possibility to reduce the noise level is e.g. to include sensor fusion of several event cameras in the payload design. The obtainment of a low noise level during the mission is also important for the usage of the Convolutional Neural Networks. While the Convolutional Neural Network architectures have demonstrated excellent results in the task of detecting and classifying objects in pictures, they still struggle with certain conditions. In particular, noisy or deform images -which might occur naturally in space due to a higher amount of high energy particles or radiation and also spacecraft tumbling- can significantly reduce the accuracy of the CNN outputs. Additionally, the success of CNNs relies fundamentally on the breadth and quality of the annotated datasets used during the supervised training process. The scarcity of datasets with event vision data recorded in space and then accurately annotated will also imply struggles in the training of the CNN models, and then a reduced prediction quality during inference time.

For the presented analysis on payload parameters and performance, we made multiple assumptions that merit additional backing. Firstly, one important assumption of the previous analysis is on the sensitivity of the event payload. This assumption contains flaws. The analysis will have to be repeated once sensitivity tests of the EventSat's event sensor have been performed. Secondly, it will not be viable to try to watch all objects at all distances, unless the payload has a variable focal length. Choosing specific targets or target areas would ease further payload development. Next topic for further work are the abilities of the ADCS subsystem and positioning system. They need to be accurately known, such that the payload can take the spacecraft pointing accuracy and positional errors into account for the focal length and field of view. Finally, EventSat's orbit should, if possible, be predetermined such that the visibility of RSO's can be better understood. This includes research in the reflectivity of objects dependent on the material and actual lighting conditions.

To refine the assumptions and to understand the limitation of the event camera, the following hardware tests are planned.

In our telescope test, the event camera is put after a Maksutov-Cassegrain telescope of 1,250 mm of focal length. This setup is to be tested on ground on a clear night. The main goal is to determine the sensitivity of the assembly in terms of magnitude and speed of movement across the field of view. Additionally, this test aims for testing the behavior of the camera outside of the controlled conditions of the lab and of screen simulations of the night sky.

We also plan for a demonstration of our event camera payload a stratospheric balloon flight. With this

Copyright ©2024 by the International Astronautical Federation (IAF). All rights reserved.

demonstration, we plan to understand the behavior and limits of the event camera in a closer space environment. The goal of the ballon flight is to record the event flow of the camera. The gathered data will support future tests and training of the Convolutional Neural Networks. During the balloon flight, the event camera will also be used to test a star tracker algorithm to assess the capacity of identification of stars in calm moments of flight but also in more animated conditions of imaging. It will then be an occasion to explore the limits of the camera and the algorithm in term of sudden and brusque motion. In addition, the data gathered will be less polluted by the motion of the atmosphere and its scattering of the light at 30 km of altitude, as well as free from additional pollution by cloud motion.

In addition to the stratospheric balloon and telescope tests, we will conduct laboratory tests of the event camera. We plan to measure the camera spectral response and limits using an optical bench. This test will be performed with calibrated light-sources and filters to find the lower limit of the sensor, where incoming light is no longer distinguishable from the sensor noise floor. Further tests to conduct are radiation and heat test of the event sensor, to identify if the sensor's perception changes once in space.

6. Conclusion

In the paper we presented in Section 3 the mission architecture of our 6U CubeSat mission, EventSat, which has an event-based payload, consisting of an event camera and a NVIDIA Jetson Orin Nano as AI onboard computer. The goal of the mission is the autonomous detection, classification, and identification of space objects to enhance Space Situational Awareness and autonomous space operations using onboard AI models which shall be reconfigurable through telecommands from ground. The presented comparison to current and planned missions, aiming for the same goal, shows that there is a need for Space Situational Awareness and Space Traffic Management systems in space, in addition to ground systems. The technological advantages of event cameras, presented in Section 2, meet the challenges resulting from Space Situational Awareness and Space Traffic Management Systems in space. The results of the preliminary payload analysis, presented in Section 4, are promising and indicate that EventSat could successfully conduct Space Situational Awareness observation despite the limiting formfactor of a 6U CubeSat platform. In the preliminary analysis we showed that the EventSat payload will be able to detect object sizes larger than 15 cm at 500km distance. The same analysis has also shown that EventSat would be able to see and detect more than 8,000 LEO objects. In addition, we identified areas for further development of the payload. The presented preliminary payload study can be seen as the basis for further in-depth study that will include the substitution of assumptions by hardware test results in an iterative process until the payload has reached the degree of maturity to be ready to be launched in space.

Acknowledgements

We are immensely grateful for the students being part of the EventSat team of the Chair of Spacecraft Systems. Their dedication, hard work and enthusiasm have been the driving force behind the progress of the EventSat CubeSat mission and exemplify the highest standards of teamwork. Thank you to each member of this extraordinary team.

References

[1] G. Gallego *et al.*, "Event-Based Vision: A Survey," *IEEE Trans Pattern Anal Mach Intell*, vol. 44, no. 1, pp. 154–180, Jan. 2022, doi: 10.1109/TPAMI.2020.3008413.

[2] A. Murtaza, S. J. H. Pirzada, T. Xu, and L. Jianwei, "Orbital Debris Threat for Space Sustainability and Way Forward (Review Article)," *IEEE Access*, vol. 8, pp. 61000–61019, 2020, doi: 10.1109/ACCESS.2020.2979505.

[3] G. Cohen, S. Afshar, A. Van Schaik, A. Wabnitz, T. Bessell, and M. Rutten, "Event-based Sensing for Space Situational Awareness," 2017. [Online]. Available: www.amostech.com

[4] N. O. Ralph, A. Marcireau, S. Afshar, N. Tothill, A. van Schaik, and G. Cohen, "Astrometric calibration and source characterisation of the latest generation neuromorphic event-based cameras for space imaging," *Astrodynamics*, vol. 7, no. 4, pp. 415–443, Dec. 2023, doi: 10.1007/s42064-023-0168-2.

[5] N. Salvatore and J. Fletcher, "Learned Event-based Visual Perception for Improved Space Object Detection."

[6] K. Xiao *et al.*, "A Preliminary Research on Space Situational Awareness Based on Event Cameras," in *2022 13th International Conference on Mechanical and Aerospace Engineering, ICMAE 2022*, Institute of Electrical and Electronics Engineers Inc., 2022, pp. 390–395. doi: 10.1109/ICMAE56000.2022.9852890.

[7] T.-J. Chin, S. Bagchi, and A. Eriksson, "Star Tracking using an Event Camera."

[8] G. Cohen, S. Afshar, and A. Van Schaik, "Approaches for Astrometry using Event-Based Sensors," 2018. [Online]. Available: www.amostech.com

[9] S. Bagchi, "Event-based Star Tracking via Multiresolution Progressive Hough Transforms."

Copyright ©2024 by the International Astronautical Federation (IAF). All rights reserved.

[10] M. Jawaid, E. Elms, Y. Latif, and T. J. Chin, "Towards Bridging the Space Domain Gap for Satellite Pose Estimation using Event Sensing," in *Proceedings - IEEE International Conference on Robotics and Automation*, Institute of Electrical and Electronics Engineers Inc., 2023, pp. 11866–11873. doi: 10.1109/ICRA48891.2023.10160531.

[11] A. Jolley, G. Cohen, D. Joubert, and A. Lambert, "Evaluation of Event-Based Sensors for Satellite Material Characterization," *J Spacecr Rockets*, vol. 59, no. 2, pp. 627–636, 2022, doi: 10.2514/1.A35015.

[12] F. Mahlknecht *et al.*, "Exploring Event Camera-Based Odometry for Planetary Robots," *IEEE Robot Autom Lett*, vol. 7, no. 4, pp. 8651–8658, Oct. 2022, doi: 10.1109/LRA.2022.3187826.

[13] O. Sikorski, D. Izzo, and G. Meoni, "Event-based spacecraft landing using time-to-contact," in *IEEE Computer Society Conference on Computer Vision and Pattern Recognition Workshops*, IEEE Computer Society, Jun. 2021, pp. 1941–1950. doi: 10.1109/CVPRW53098.2021.00222.

[14] "World's First Neuromorphic Sensor Launched to Space – iniVation." Accessed: Sep. 10, 2024. [Online]. Available: https://inivation.com/worlds-first-neuromorphic-sensor-launched-to-space/

[15] "From Western Sydney University to orbit: stellar new camera tech on the International Space Station | Western Sydney University." Accessed: Sep. 10, 2024. [Online]. Available: https://www.westernsydney.edu.au/newscentre/news_centre/more_news_stories/from_western_sydney_university_to_orbit_stellar_new_camera_tech_on_the_international_space_station

[16] "Space Environment Statistics · Space Debris User Portal." Accessed: Sep. 16, 2024. [Online]. Available: https://sdup.esoc.esa.int/discosweb/statistics/

[17] "Discovery Statistics." Accessed: Sep. 16, 2024. [Online]. Available: https://cneos.jpl.nasa.gov/stats/totals.html

[18] M. Ghiglione and V. Serra, "Opportunities and challenges of AI on satellite processing units," in *ACM International Conference Proceeding Series*, Association for Computing Machinery, May 2022, pp. 221–224. doi: 10.1145/3528416.3530985.

[19] J. M. Réaltra, J. E. Ward, and B. Mac Namee, "Developing Machine Learning Models for Space Based Edge AI Platforms." [Online]. Available: https://colab.research.google.com

[20] W. Shariff, M. A. Farooq, J. Lemley, and P. Corcoran, "Event-based YOLO Object Detection: Proof of Concept for Forward Perception System."

[21] J. Redmon, S. Divvala, R. Girshick, and A. Farhadi, "You Only Look Once: Unified, Real-Time Object Detection," Jun. 2015, [Online]. Available: http://arxiv.org/abs/1506.02640

[22] S. A. Nawaz, J. Li, U. A. Bhatti, M. U. Shoukat, and R. M. Ahmad, "AI-based object detection latest trends in remote sensing, multimedia and agriculture applications," Nov. 18, 2022, *Frontiers Media S.A.* doi: 10.3389/fpls.2022.1041514.

[23] NVIDIA, "NVIDIA Jetson Nano," https://www.nvidia.com/en-us/autonomous-machines/embedded-systems/jetson-nano/product-development/.

[24] "Starlink satellites: Facts, tracking and impact on astronomy | Space." Accessed: Aug. 27, 2024. [Online]. Available: https://www.space.com/spacex-starlink-satellites.html

[25] "OneWeb Minisatellite Constellation - eoPortal." Accessed: Aug. 27, 2024. [Online]. Available: https://www.eoportal.org/satellite-missions/oneweb

[26] "What is 'Project Kuiper,' Amazon's New Satellite Internet Initiative?" Accessed: Aug. 27, 2024. [Online]. Available: https://www.aboutamazon.com/news/innovation-at-amazon/what-is-amazon-project-kuiper

[27] T. Flohrer and H. Krag, "SPACE SURVEILLANCE AND TRACKING IN ESA'S SSA PROGRAMME", Accessed: Aug. 27, 2024. [Online]. Available: http://spacedebris2017.sdo.esoc.esa.int,

[28] "NorthStar - Satellite Constellation - NewSpace Index." Accessed: Aug. 27, 2024. [Online]. Available: https://www.newspace.im/constellations/northstar

[29] "Vyoma orders pilot satellites for debris-monitoring constellation - SpaceNews." Accessed: Aug. 27, 2024. [Online]. Available: https://spacenews.com/vyoma-orders-pilot-satellites-for-debris-monitoring-constellation/

[30] "Aerospacelab to build debris-tracking satellite for Vyoma - SpaceNews." Accessed: Aug. 27, 2024. [Online]. Available: https://spacenews.com/aerospacelab-to-build-debris-tracking-satellite-for-vyoma/

[31] M. Graziano, A. Tomassini, and J. Naudet, "SBSS-DM and ANDROID: two small missions for Space-Based Space Surveillance and Active Debris Removal Demonstrations", doi: 10.13009/EUCASS2017-631.

Copyright ©2024 by the International Astronautical Federation (IAF). All rights reserved.

[32] "Skylark (Lemur-2) Satellites - Nanosats Database." Accessed: Aug. 27, 2024. [Online]. Available: https://www.nanosats.eu/sat/lemur-2-northstar

[33] "ENDURANCE-15 Platform - EnduroSat." Accessed: Aug. 27, 2024. [Online]. Available: https://www.endurosat.com/products/endurance-15-platform/

[34] "Products | Aerospacelab." Accessed: Aug. 27, 2024. [Online]. Available: https://www.aerospacelab.com/products

[35] W. E. Krag, "AD-785 380 VISIBLE MAGNITUDE OF TYPICAL SATELLITES IN SYNCHRONOUS ORBITS."

[36] M. Zolnowski *et al.*, "Observational Evaluation of Event Cameras Performance in Optical Space Surveillance." [Online]. Available: https://www.researchgate.net/publication/330652072

[37] "Jonathan's Space Report | GCAT." Accessed: Sep. 25, 2024. [Online]. Available: https://planet4589.org/space/gcat/

[38] R. Wang, J. Liu, and Q. M. Zhang, "Propagation errors analysis of TLE data," *Advances in Space Research*, vol. 43, no. 7, pp. 1065–1069, Apr. 2009, doi: 10.1016/j.asr.2008.11.017.

[39] "Event-based Vision Sensor (EVS) | Image Sensor for Industrial Use [Overview] | Image Sensor | Products & Solutions | Sony Semiconductor Solutions Group." Accessed: Sep. 16, 2024. [Online]. Available: https://www.sony-semicon.com/en/products/is/industry/evs.html

[40] "Home · Space Debris User Portal." Accessed: Sep. 16, 2024. [Online]. Available: https://sdup.esoc.esa.int/